

Sub-optical-cycle electron dynamics of NO molecules: the effect of strong laser field and Coulomb field

Wenhui Hu, Xing Li, Hongxue Zhao, Wankai Li, Yue Lei, Xiangzheng Kong, Aihua Liu, Sizuo Luo  and Dajun Ding

Institute of Atomic and Molecular Physics, Jilin University, Changchun 130012, People's Republic of China

E-mail: luosz@jlu.edu.cn and dajund@jlu.edu.cn

Received 24 October 2019, revised 10 January 2020

Accepted for publication 27 January 2020

Published 16 March 2020



CrossMark

Abstract

The sub-cycle bound- and free-electron dynamics and the Coulomb effect during the strong field ionization of NO molecules are studied by using a combination of phase-controlled two-color femtosecond laser fields and photoelectron imaging. The AC–Stark effect and ponderomotive potential is identified and tracked by measuring the energy shift of phase-dependent photoelectron spectra under different asymmetric laser fields. The Coulomb effects of molecules during ionization are studied by measuring the energy-dependent phase change and the cusp-like transverse-momentum distributions of the ionized electrons. The results show an obvious sub-cycle time scale response of ionized electrons in NO molecular ionization. The present method provides new ways to measure the electronic dynamics of molecules in strong field ionization.

Keywords: sub-optical-cycle electron dynamics, AC–Stark effect, Coulomb effect

(Some figures may appear in colour only in the online journal)

1. Introduction

The interaction of strong laser fields with atoms/molecules causes multiphoton ionization, tunneling ionization, high-order harmonic generation and non-sequential double ionization and shows us the attosecond time evolution of the world [1]. Besides modifying the shape of Coulomb potential, strong laser fields can change the energy of targets, i.e., AC–Stark energy shift and ponderomotive potential of bound and free electrons, respectively [2–6]. Thus, understanding the influence of laser field manipulation is essential for the strong field ionization of atoms and molecules. However, the AC–Stark effect of bound electrons and the ponderomotive potential of free electrons were confirmed by their cycle-averaged effects only in general by measuring the laser wavelength or intensity-dependent absorption or photoelectron spectra [7–9], even though the AC–Stark shift and ponderomotive potential originate from the bound- and free-electron dynamics induced by the sub-cycle electric field of a laser. Experiments have shown an average response time of

~10 fs for the AC–Stark shift in the few cycle laser pump–probe measurements [10, 11]. Though the sub-cycle AC–Stark shifts of atom energy levels has been probed with attosecond XUV absorption measurement [12, 13], these effects from the change of target energy should be investigated further to explore the instantaneous appearance and periodical influences of electronic dynamics during ionization by laser fields. Therefore, we propose that if the laser field were manipulated within the optical cycle, the sub-cycle response of the AC–Stark effect and ponderomotive potential could be tracked through measuring the phase-dependent photoelectron spectra during strong field ionization. Moreover, the influences of the Coulomb effect on atoms/molecules in the trajectories of ionized electrons can also be illustrated more clearly in the manipulated laser fields though the final electron momentum during strong field ionization. In fact, the final electron momentum is only related to the vector potential of the electric field if one considers it in simple terms and without the effect of Coulomb potential [14]. Recently, several studies have shown the important contribution of the

Coulomb effect during strong field ionization in Coulomb focusing, low-energy electron generation, Rydberg excitation of atoms/molecules, electron rotation during atto-clock measurement, and so on [15–19]. Thus, the actual final momentum of ionized electrons is not only related to the field vector potential, but also influenced by the Coulomb potential during the propagation. Particularly, it is found that the electrons after tunneling are focused by the Coulomb potential and an obvious cusp-like structure is produced in their momentum distribution [20, 21]. It is clear that the influence of the Coulomb potential on the electron momentum distribution should be directly related to different symmetric properties of the electrons in molecules and leads to the suppression of ionization and the interference of electron wavepackets [22–24] as different sub-cycle interferences can appear between the rescattering and direct electron wavepackets under the influence of Coulomb potential [25–28].

The nitric oxide (NO) molecule has been chosen as the sample in our experiment since it is a benchmark one for studying the strong field ionization of molecular systems [29–34]. Many related studies have been focused on the cycle-averaged AC–Stark effect during NO ionization [35–39]. Ludowise *et al* studied the time-resolved photoionization of NO in intense femtosecond laser fields and found that its potential energy curve was distinctly disturbed and that the measured energy peaks shifted when changing the laser intensity [30]. Lopez-Martens *et al* confirmed the averaged AC–Stark shift of the NO potential energy curve by measuring the fluorescence under different femtosecond laser intensities [31]. Recently, we explored the effect of coherent interference between electronic states on the ionization of NO molecules by intense ultrafast two-color laser pulses, and the results prove that the AC–Stark effects also play a role and can modulate the interference patterns in the electron spectra due to the multiphoton and multi-pathway ionizations [40, 41]. When a monochromatic femtosecond laser with long pulse duration is used, most of the ionization response in sub-cycle is averaged by the symmetric field; however, a phase-controlled two-color laser can distinguish the electron dynamics on an attosecond time scale experimentally. Thus, in this work, we have studied the effect of a sub-cycle laser field and Coulomb potential on bound and free electrons during the strong field ionization of NO molecules by using phase-controlled two-color femtosecond laser fields combined with the photoelectron imaging method. The sub-cycle AC–Stark effect and ponderomotive potential were confirmed by measuring the phase-dependent photoelectron energy spectra and the observed energy shift of electrons was related to the asymmetry of the two-color laser fields. The Coulomb effect during the strong field ionization of molecules was also illustrated by measuring the energy-dependent phase shift and transverse-momentum distribution of electrons. It was found that the observed cusp-like transverse-momentum distribution was caused by Coulomb focusing and also depended on the laser field.

2. Experimental setup

Our experimental setup consists of a velocity map imaging spectrometer (VMIS) [42], a phase-controlled two-color

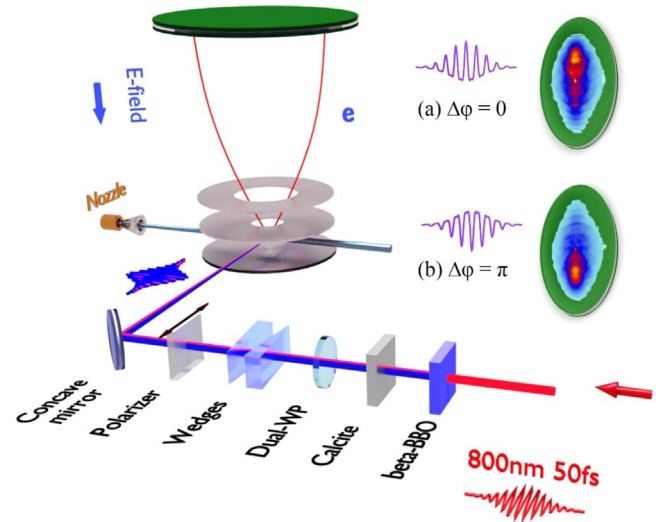


Figure 1. Schematic diagram of the experimental setup for the photoelectron images of NO molecules from two-color laser ionization with controlled relative phases.

femtosecond laser field and a supersonic NO molecular beam, as shown in figure 1. The details can be found in our previous papers [40, 41, 43]. Briefly, the linearly polarized fundamental 800 nm laser (ω) is generated from a commercial chirped pulse amplified (CPA) Ti:sapphire laser system with 1 kHz repetition rate, 50 fs pulse duration (full width at half maximum) and 4 mJ per pulse. Its second harmonic 400 nm laser field (2ω) is produced after passing through a β -BBO. The polarizations of ω and 2ω fields are rotated to the same direction by a dual-wavelength wave plate. A two-color laser field with $E(t) = E_{\omega}f(t)\cos(\omega t) + E_{2\omega}f(t)\cos(2\omega t + \Delta\varphi)$ can be generated from these ω and 2ω lights when they pass a wire grid polarizer, where $E_{\omega,2\omega}$ stands for the amplitude of the electric field for ω and 2ω lasers, $f(t)$ denotes the pulse envelope, $\Delta\varphi$ is the relative phase between two laser fields in steps of 0.08π (about 110 as according to the 2.67 fs of a 2π period to 800 nm laser) which can be controlled via moving a pair of wedges mounted on a high-precision translation stage. After that, a spherical mirror with $f = 30$ cm focuses the synthetic two-color laser beam into the vacuum chamber to interact with the molecular beam (1% NO in neon), ejected by a pulsed piezo-valve (ACPV2 [44]). The ionizing electrons are collected in the VMIS and imaged onto a microchannel plate–phosphor screen assembly. The imaging data from the charge-coupled device camera is sent to a computer for further processing. The relative phase between the two-color laser fields is calibrated by measuring the asymmetric momentum distribution of S^+ from the Coulomb explosion of OCS molecules by comparing with the previous measurement [45]. For extracting the electron momentum distribution, each measured image is separated into a left and a right part along the polarization and the Abel inversion is performed by using the Basex method [46]. The intensity calibration for both ω and 2ω lasers is given by measuring the Stark shift of the electron energy spectra of xenon [47, 48].

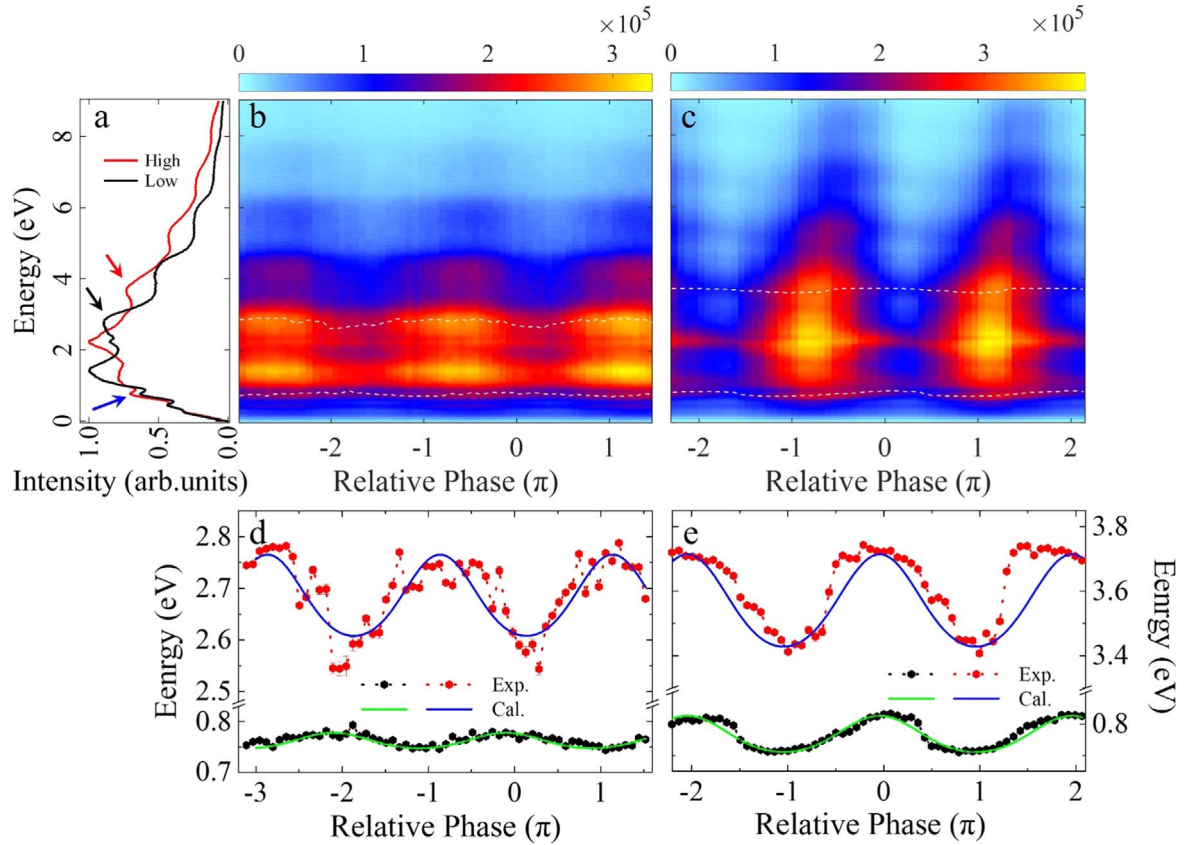


Figure 2. Energy spectra of the electrons on the one side of the detector generated from a phase-controlled two-color laser field interacting with molecules at the laser intensity of 800 nm ($5.3 \times 10^{13} \text{ W cm}^{-2}$) with different 400 nm intensity: (b) low, $4.4 \times 10^{12} \text{ W cm}^{-2}$; (c) High, $7.4 \times 10^{12} \text{ W cm}^{-2}$. The black and red lines in (a) are the phase-averaged energy spectra from the low and high asymmetric fields, respectively. The white dotted lines in (b) and (c) indicate that the energy of corresponding peaks is varying with the relative phase in different asymmetric fields, and the experiment and calculation results are plotted in (d) and (e).

3. Results and discussions

The ionized electron distributions on two sides of the detector along the polarization direction are modulated by adjusting the relative phase of the two-color laser field and these distributions from the two sides are varied by a π phase difference. The measured electron energy spectra on the one side of the detector as a function of the relative phase between the two-color laser fields are plotted in figure 2. The phase-averaged electron spectra in the two-color laser fields with different asymmetry are displayed in figure 2(a). For the Keldysh parameter corresponding to the laser intensity used in this paper (dominant by the 800 nm component) is around 1, according to the general point of view in strong field physics, there is both a multiphoton ionization mechanism and a tunneling-ionization mechanism in this laser intensity region [49]. The blue arrow indicates the narrow peak from Freeman resonance, which is centered at 0.76 eV and does not shift in both laser conditions, and this peak is generated from the ionization of the $A^2\Sigma^+$ and $B^2\Pi$ Rydberg states [40]. The black and red arrows indicate the broaden peaks around 2.68 eV and 3.60 eV from the non-resonant second above-threshold ionization (ATI) by different asymmetric two-color laser fields, their shifted first order ATI peaks at 1.1 eV and 2.1 eV in two laser intensities are also observed. Figures 2(b)

and (c) show the results obtained in the two-color laser fields with the same intensity of 800 nm laser ($5.3 \times 10^{13} \text{ W cm}^{-2}$) but different 400 nm laser intensity at $4.4 \times 10^{12} \text{ W cm}^{-2}$ (low) and $7.4 \times 10^{12} \text{ W cm}^{-2}$ (high), respectively.

One can see from these results that the distinct energy oscillation originated from the sub-cycle response of bound- and free-electron dynamics in strong field NO ionization. Firstly, the peak energy of the electrons from resonance enhanced multiphoton ionization (REMPI) and tunneling ionization changes with tuning the relative phase, as marked by white dashed lines in figures 2(b) and (c). These data are also shown in figures 2(d) and (e) for comparing them to the simple calculation from the E_U in equation (1) of a two-color laser field. They clearly indicate a cyclical oscillation with a 2π period for both the energies of the electrons, which coincided with the expectation of the modulation of the synthesized laser electric field. Next, the sensitivity of the energy shifts to REMPI and direct-tunneling ionization is quite different. The energy oscillation amplitude for REMPI is much smaller than that for the direct-tunneling ionization. Both the amplitudes increase with increasing the asymmetry of two-color laser field, that is, the amplitude of energy oscillation is 0.01 eV for the 0.76 eV energy peak and 0.08 eV for the 2.68 eV energy peak at low asymmetry while they increase to 0.06 eV and 0.15 eV for the 0.76 eV and 3.60 eV

energy peaks, respectively, at high asymmetry. The fact that the energy shifts for direct-tunneling ionization are more sensitive to the relative phase is due to the change of total ponderomotive potential for the relative phase and the dependence of the ionization moment, and the energy of the direct electrons averaged over an optical cycle at the instant of ionization t_0 in the two-color field can be written as [50]

$$E_U = U_{P1} + 2U_{P1} \sin^2 \omega t + U_{P2} + 2U_{P2} \sin^2 (2\omega t + \varphi) + 4\sqrt{U_{P1}U_{P2}} \sin \omega t_0 \sin (2\omega t_0 + \varphi), \quad (1)$$

where the ponderomotive energy is $U_{pi} = e^2 \mathcal{E}^2 / 4m\omega^2$ ($i = 1, 2$ represent the ω and 2ω laser fields). The calculated energy shifts for the direct ionized electron from equation (1) agree very well with the measured data, as shown by the blue lines in figures 2(e) and (f). It confirms that the sub-cycle response of the ponderomotive potential contributes to the shifts of these electron energies.

For the bound electrons, we can refer to the phase-dependent electron energy shift as the contribution of sub-cycle AC-Stark effect. It is known that the energy levels of molecular bound states can be modified by strong laser field through the AC-Stark effect and, for a symmetric laser field, the cycle's averaged AC-Stark shift can be described as

$$\delta E = -\frac{1}{4} \alpha(\omega) \varepsilon_0^2 \propto -\alpha(\omega) I, \quad (2)$$

with $\alpha(\omega)$ the polarizability and I the laser intensity of a two-color laser. Due to the change of the electric field for the specified direction as relative phase the tuned, the energy level shifts at the sub-cycle representation should be performed analytically for multicycle pulses [13]

$$\delta E = \frac{1}{2} \varepsilon(t)^2 [\alpha \cos^2(\omega t) - i\gamma \sin(2\omega t)], \quad (3)$$

where γ is the sub-cycle change in the population of states coupling and the instantaneous electric field, $\varepsilon(t)$, for a two-color laser can be written as

$$E(t) = \mathcal{E}_\omega f(t) \cos(\omega t) + \mathcal{E}_{2\omega} f(t) \cos(2\omega t + \Delta\varphi). \quad (4)$$

with \mathcal{E}_ω , $\mathcal{E}_{2\omega}$ the electric field amplitude for 800 and 400 nm lasers, respectively. Though the polarizability and the sub-cycle changes in the population of states coupling cannot be obtained in this calculation, the observed kinetic energy of these photoelectrons from REMPI can be given simply by

$$E_k = q\hbar\omega - (I_p - E_R) - (1 - \lambda)U_p, \quad (5)$$

where q is the photon number of absorption for ionization from the resonant state, I_p is the ionization energy of molecules, E_R is the energy of resonant state, U_p is the total ponderomotive potential from two-color laser fields. λ scales the ratio of the AC-Stark shift of the resonant states to the ponderomotive energy [31, 51], and one can obtain the λ for the low-asymmetry laser fields by fitting the measured results in figure 2(d) by the calculation from equation (5). It leads to a λ value of 0.82 for low asymmetric laser fields, which agrees

well with our previous results [40], and 0.6 for high asymmetric laser fields, which can be assigned to other resonance state involved in REMPI.

It is noteworthy that the phase corresponding to the energy maximum in a 2π period also changes with the different energetic electrons from ionization. We assign this change to the effect of the Coulomb field in the molecules on these ionized electrons. To clarify it, we plot the measured asymmetric parameters, $A(E, \Delta\varphi) = \frac{Left(E, \Delta\varphi) - Right(E, \Delta\varphi)}{Left(E, \Delta\varphi) + Right(E, \Delta\varphi)}$, as a function of the relative phase in figures 3(a) and (b). We also give the variation of the asymmetric parameters for different ATI peaks (second to fifth order) when tuning the relative phase in figures 3(c) and (d). The relationships for the amplitudes of the parameter variation and the relative phases with the electron energy are given in figures 3(e) and (f), respectively. For the low asymmetric field the amplitudes close to 0.2 in the energy range, and almost 0.4 for the high asymmetric field. The results show that the field asymmetry has a strong influence on the amplitudes. It can be understood as the sub-cycle ionization probability changes with the field profile caused by varying the relative phase. The amplitude becomes larger for ionization of high asymmetric fields since the ionization probability has an exponential dependence on the laser intensity. The relative phase changes with different orders of ATI peaks are shown in figure 3(f), which increases as the increase of the electron energy. The trends of both the low and high asymmetric fields are almost the same, indicating the inherent feature of the long-range Coulomb effect for atoms/molecules [52, 53]. As the ionization time is sensitive to the profile of the electric field [54, 55], the observed sub-cycle ionization by tuning the relative phase of the two-color field can provide a tool for further exploring the attosecond evolution of an electron wavepacket during the strong field ionization of molecules.

The transverse-momentum distributions are measured at different relative phases for the high asymmetric field. It shows quite different distributions when varying the relative phases, as can be seen in figures 4(a) and (b). The cusp-like structure for the transverse momentum is observed due to the focusing of the molecular Coulomb potential, like the case for atoms. For example, figure 4(c) gives the profile comparison for the values -0.9π and 0.1π of relative phases corresponding to the maximum and minimum signal intensities. The distribution for -0.9π is a typical cusp, while the distribution for 0.1π is much narrower for the small momenta, <0.08 a.u., and broader for the large momenta, >0.08 a.u. The change of transverse momentum may be generated by the retrapped ionization of molecules, which is derived from the different trajectories of electrons under the influence of the Coulomb field [56]. To explain these observations in a molecule target, more theoretical simulations are certainly required since the real situation is much more complex and one should consider more factors in this ultrafast laser ionization of molecules, such as the initial transverse and longitudinal momentum distributions of the ionized electrons, which are quite different under different shaped laser fields, the tunneling point for different laser intensity, the interference

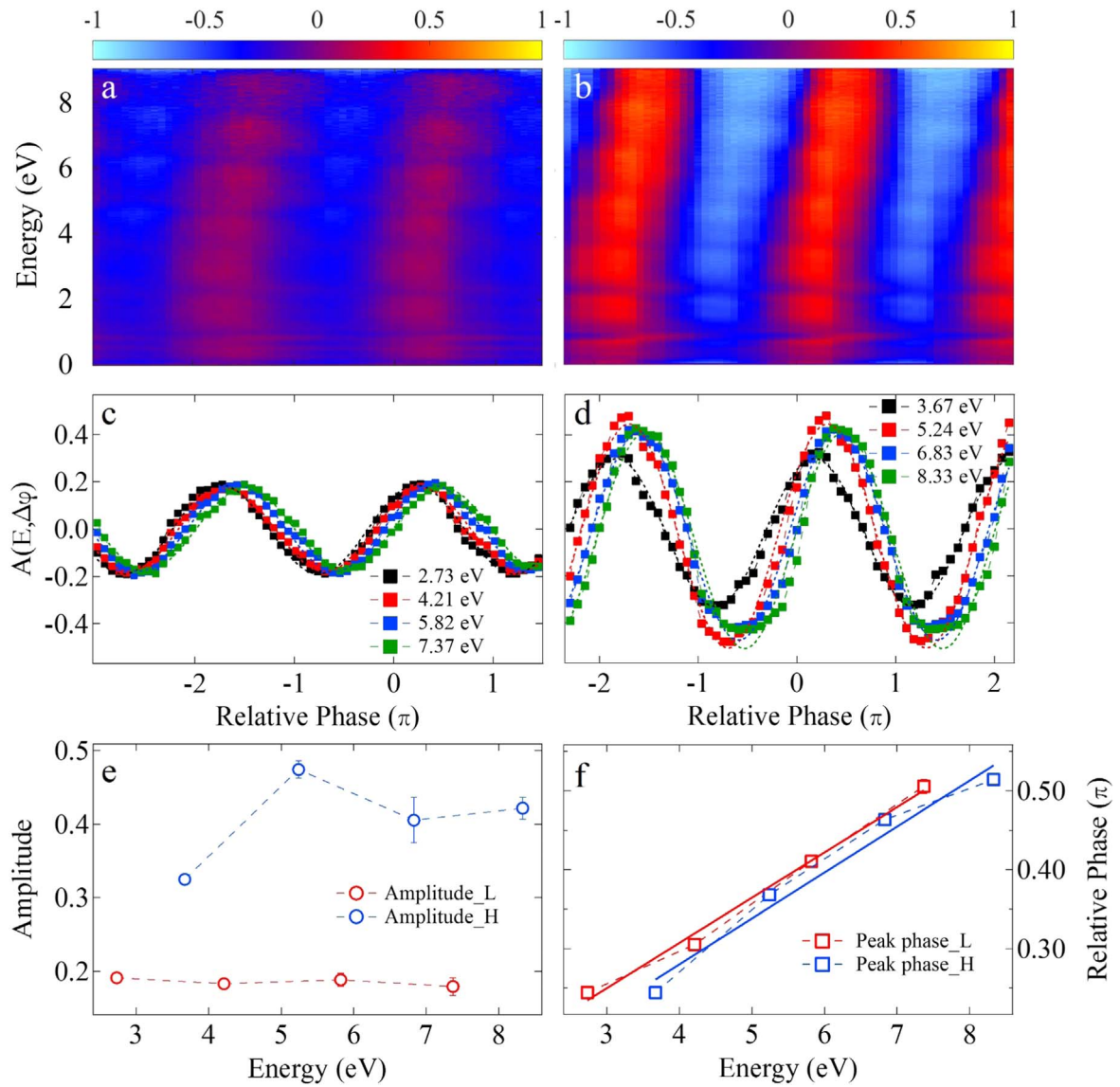


Figure 3. (a) and (b) Measured asymmetry parameter $A(E, \Delta\varphi)$ and its modulation of energy-resolved ATI electron peaks under the asymmetric two-color laser field with different 400 nm intensity. (c) and (d) Measured asymmetry for different ATI peaks at low and high asymmetry laser fields. (e) and (f) Corresponding modulated amplitude and phase of the ATI peaks from two laser conditions.

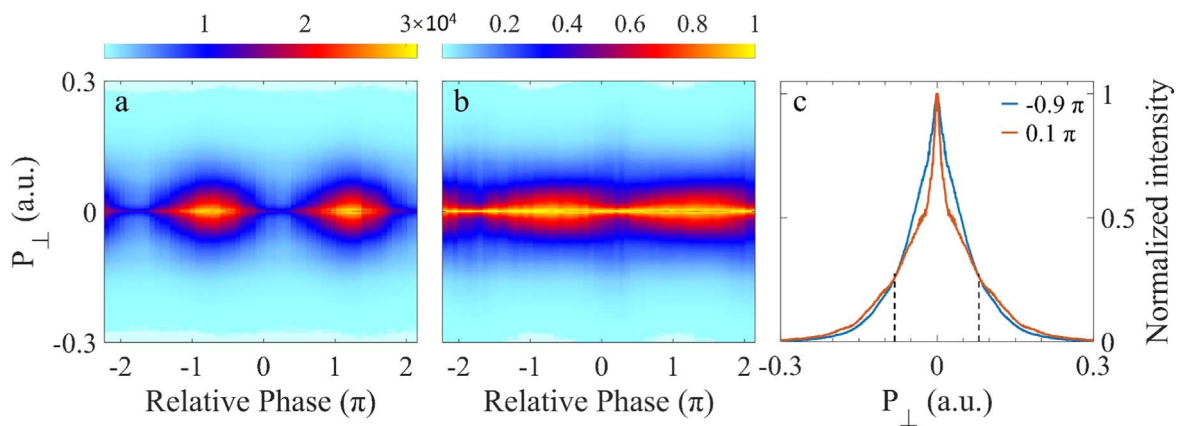


Figure 4. (a) Phase-dependent transverse-momentum distribution of electrons measured on the one side of a detector under the laser intensity of 800 nm ($5.3 \times 10^{13} \text{ W cm}^{-2}$) and 400 nm ($7.4 \times 10^{12} \text{ W cm}^{-2}$). (b) The corresponding normalized transverse-momentum distributions. (c) The comparison of transverse momentum obtained at the relative phase of -0.9π and 0.1π , the black dotted lines indicate the momenta about ± 0.08 a.u.

between electron wavepackets, etc. For example, if one believes that the electronic momentum is determined by its initial value, it may be reasonable to establish a similar discussion with the ionization under the laser fields with different intensity, that is, for electrons with small initial momenta, the Coulomb focusing is stronger because these electrons should stay much longer in the Coulomb potential. On the other hand, electrons with large initial momenta only have a small probability to be driven back by the laser field to the nucleus and, therefore, the Coulomb focusing is weak, they will keep the larger transverse momentum and broaden the contribution.

4. Summary

Tracking the sub-cycle energy level modification of molecules and electron dynamics in strong laser fields is quite important in attosecond physics. We have experimentally studied the sub-cycle dynamics of bound and free electrons during the strong field ionization of NO molecules in phase-controlled two-color femtosecond laser fields. The sub-cycle AC–Stark effect and ponderomotive potential are identified from the measured energy shift of phase-dependent photoelectron spectra. The Coulomb effects during strong field ionization are traced by measuring the phase change with ATI electron energy and the transverse-momentum distributions of the ionized electrons. The observed phase changes and cusp-like transverse-momentum distributions illustrate that the Coulomb effect makes a significant contribution during the strong field ionization of NO molecules. Our experiments provide a new ways to explore the electronic dynamics of molecular ionization in intense laser fields.

Acknowledgments

This work was supported by the National Natural Science Foundation of China (NNSFC) (11534004, 11704148, 11627807, 11774131) and the Science Challenge Project (No. TZ2018005).

ORCID iDs

Sizuo Luo  <https://orcid.org/0000-0002-8969-5958>

References

- [1] Krausz F and Ivanov M 2009 Attosecond physics *Rev. Mod. Phys.* **81** 163–234
- [2] Delone N B and Krainov V P 1999 AC Stark shift of atomic energy levels *Physics—Uspekhi* **42** 669–87
- [3] Bucksbaum P H, Freeman R R, Bashkansky M and McIlrath T J 1987 Role of the ponderomotive potential in above-threshold ionization *J. Opt. Soc. Am. B* **4** 760
- [4] Muller H, Tip A and Van der Wiel M 1983 Ponderomotive force and AC Stark shift in multiphoton ionisation *J. Phys. B: At. Mol. Phys.* **16** L679
- [5] Sussman B J 2011 Five ways to the nonresonant dynamic Stark effect *Am. J. Phys.* **79** 477
- [6] Demekhin P V and Cederbaum L S 2012 Dynamic interference of photoelectrons produced by high-frequency laser pulses *Phys. Rev. Lett.* **108** 253001
- [7] Kruit P, Kimman J, Muller H and Van der Wiel M 1983 The AC Stark shift as an intensity probe in resonant multiphoton ionisation of xenon *J. Phys. B: At. Mol. Phys.* **16** 937–49
- [8] Freeman R R and Bucksbaum P H 1991 Investigations of above-threshold ionization using subpicosecond laser pulses *J. Phys. B: At. Mol. Opt. Phys.* **24** 325–47
- [9] Mitroy J, Safronova M S and Clark C W 2010 Theory and applications of atomic and ionic polarizabilities *J. Phys. B: At. Mol. Opt. Phys.* **43** 202001
- [10] Mysyrowicz A, Hulin D, Antonetti A, Migus A, Masselink W T and Morkoc H 1986 ‘Dressed excitons’ in a multiple-quantum-well structure: evidence for an optical Stark effect with femtosecond response time *Phys. Rev. Lett.* **56** 2748–51
- [11] Becker P C, Fork R L, Brito Cruz C H, Gordon J P and Shank C V 1988 Optical Stark effect in organic dyes probed with optical pulses of 6-fs duration *Phys. Rev. Lett.* **60** 2462–4
- [12] Wirth A *et al* 2011 Synthesized light transients *Science* **334** 195–200
- [13] Chini M, Zhao B, Wang H, Cheng Y, Hu S X and Chang Z 2012 Subcycle ac stark shift of helium excited states probed with isolated attosecond pulses *Phys. Rev. Lett.* **109** 073601
- [14] Corkum P B 1993 Plasma perspective on strong field multiphoton ionization *Phys. Rev. Lett.* **71** 1994–7
- [15] Brabec T, Ivanov M Y and Corkum P B 1996 Coulomb focusing in intense field atomic processes *Phys. Rev. A* **54** R2551–4
- [16] Blaga C I, Catoire F, Colosimo P, Paulus G G, Muller H G, Agostini P and DiMauro L F 2009 Strong-field photoionization revisited *Nat. Phys.* **5** 335–8
- [17] Sainadh U S, Xu H, Wang X, Atia-Tul-Noor A, Wallace W C, Douguet N, Bray A, Ivanov I, Bartschat K and Kheifets A 2019 Attosecond angular streaking and tunnelling time in atomic hydrogen *Nature* **568** 75–7
- [18] Smirnova O, Spanner M and Ivanov M 2006 Coulomb and polarization effects in sub-cycle dynamics of strong-field ionization *J. Phys. B: At. Mol. Opt. Phys.* **39** S307
- [19] Sabbar M, Timmers H, Chen Y-J, Pymar A K, Loh Z-H, Sayres Scott G, Pabst S, Santra R and Leone S R 2017 State-resolved attosecond reversible and irreversible dynamics in strong optical fields *Nat. Phys.* **13** 472
- [20] Comtois D, Zeidler D, Pepin H, Kieffer J C, Villeneuve D M and Corkum P B 2005 Observation of Coulomb focusing in tunnelling ionization of noble gases *J. Phys. B: At. Mol. Opt. Phys.* **38** 1923–33
- [21] Arbo D G, Miraglia J E, Gravielle M S, Schiessl K, Persson E and Burgdorfer J 2008 Coulomb-Volkov approximation for near-threshold ionization by short laser pulses *Phys. Rev. A* **77** 013401
- [22] Posthumus J H 2004 The dynamics of small molecules in intense laser fields *Rep. Prog. Phys.* **67** 623–65
- [23] Miller M R, Xia Y, Becker A and Jaron-Becker A 2016 Laser-driven nonadiabatic electron dynamics in molecules *Optica* **3** 259–69
- [24] Nisoli M, Decleva P, Calegari F, Palacios A and Martin F 2017 Attosecond electron dynamics in molecules *Chem. Rev.* **117** 10760–825
- [25] Huismans Y *et al* 2011 Time-resolved holography with photoelectrons *Science* **331** 61–4
- [26] Shvetsov-Shilovski N I and Lein M 2018 Effects of the Coulomb potential in interference patterns of strong-field holography with photoelectrons *Phys. Rev. A* **97** 013411
- [27] Porat G *et al* 2018 Attosecond time-resolved photoelectron holography *Nat. Commun.* **9** 2805

- [28] Maxwell A S, Al-Jawahiry A, Lai X Y and Faria C F D 2018 Analytic quantum-interference conditions in Coulomb corrected photoelectron holography *J. Phys. B: At. Mol. Opt. Phys.* **51** 044004
- [29] Miller J C and Compton R N 1981 Multiphoton ionization photoelectron spectroscopy of nitric oxide *J. Chem. Phys.* **75** 22–9
- [30] Ludowise P, Blackwell M and Chen Y 1996 Perturbation of electronic potentials by femtosecond pulses—time resolved photoelectron spectroscopic study of NO multiphoton ionization *Chem. Phys. Lett.* **258** 530–9
- [31] Lopez-Martens R B, Schmidt T W and Roberts G 2000 ac Stark shifts in Rydberg NO levels induced by intense laser pulses *Phys. Rev. A* **62** 013414
- [32] Wang B X, Liu B K, Wang Y Q and Wang L 2010 Field modulation of Rydberg-state populations of NO studied by femtosecond time-resolved photoelectron imaging *Phys. Rev. A* **81** 043421
- [33] Li H, Ray D, De S, Znakovskaya I, Cao W, Laurent G, Wang Z, Kling M F, Le A T and Cocke C L 2011 Orientation dependence of the ionization of CO and NO in an intense femtosecond two-color laser field *Phys. Rev. A* **84** 043429
- [34] Endo T, Matsuda A, Fushitani M, Yasuike T, Tolstikhin O I, Morishita T and Hishikawa A 2016 Imaging electronic excitation of NO by ultrafast laser tunneling ionization *Phys. Rev. Lett.* **116** 163002
- [35] Dove T, Schmidt T W, Lopez-Martens R B and Roberts G 2001 Optical control of electronic state populations via the dynamic Stark effect *Chem. Phys.* **267** 115–29
- [36] Lopez-Martens R B, Schmidt T W and Roberts G 2002 Time-resolved Stark effect in rapidly varying fields *Appl. Phys. B* **74** 577–81
- [37] Sun Z G, Liu H P, Lou N Q and Cong S L 2003 Selecting ionization path by dynamic Stark shift with strong laser pulse *Chem. Phys. Lett.* **369** 374–9
- [38] Schmidt T W, López-Martens R B and Roberts G 2004 Time-resolved spectroscopy of the dynamic Stark effect *J. Phys. B: At. Mol. Opt. Phys.* **37** 1125–40
- [39] Trallero-Herrero C, Cardoza D, Weinacht T C and Cohen J L 2005 Coherent control of strong field multiphoton absorption in the presence of dynamic Stark shifts *Phys. Rev. A* **71** 013423
- [40] Hu W H, Liu Y, Luo S Z, Li X, Yu J Q, Li X K, Sun Z G, Yuan K J, Bandrauk A D and Ding D J 2019 Coherent interference of molecular electronic states in NO by two-color femtosecond laser pulses *Phys. Rev. A* **99** 011402
- [41] Liu Y, Hu W, Luo S, Yuan K-J, Sun Z, Bandrauk A D and Ding D 2019 Vibrationally resolved above-threshold ionization in NO molecules by intense ultrafast two-color laser pulses: an experimental and theoretical study *Phys. Rev. A* **100** 023404
- [42] Eppink A T J B and Parker D H 1997 Velocity map imaging of ions and electrons using electrostatic lenses: application in photoelectron and photofragment ion imaging of molecular oxygen *Rev. Sci. Instrum.* **68** 3477–84
- [43] Yu J Q, Hu W H, Li X K, Ma P, He L H, Liu F C, Wang C C, Luo S Z and Ding D J 2017 Contribution of resonance excitation on ionization of OCS molecules in strong laser fields *J. Phys. B: At. Mol. Opt. Phys.* **50** 235602
- [44] Irimia D, Dobrikov D, Kortekaas R, Voet H, van den Ende D A, Groen W A and Janssen M H 2009 A short pulse (7 micros FWHM) and high repetition rate (dc-5 kHz) cantilever piezovalve for pulsed atomic and molecular beams *Rev. Sci. Instrum.* **80** 113303
- [45] Ohmura H, Saito N and Morishita T 2014 Molecular tunneling ionization of the carbonyl sulfide molecule by double-frequency phase-controlled laser fields *Phys. Rev. A* **89** 013405
- [46] Dribinski V, Ossadtschi A, Mandelshtam V A and Reisler H 2002 Reconstruction of Abel-transformable images: the Gaussian basis-set expansion Abel transform method *Rev. Sci. Instrum.* **73** 2634–42
- [47] Li M, Zhang P, Luo S, Zhou Y, Zhang Q, Lan P and Lu P 2015 Selective enhancement of resonant multiphoton ionization with strong laser fields *Phys. Rev. A* **92** 063404
- [48] Huter O and Temps F 2017 Note: energy calibration of a femtosecond photoelectron imaging detector with correction for the ponderomotive shift of atomic ionization energies *Rev. Sci. Instrum.* **88** 046101
- [49] Popruzhenko S V 2014 Keldysh theory of strong field ionization: history, applications, difficulties and perspectives *J. Phys. B: At. Mol. Opt. Phys.* **47** 204001
- [50] Schumacher D W and Bucksbaum P H 1996 Phase dependence of intense-field ionization *Phys. Rev. A* **54** 4271–8
- [51] Fillion-Gourdeau F, Lorin E and Bandrauk A D 2012 Relativistic Stark resonances in a simple exactly soluble model for a diatomic molecule *J. Phys. A: Math. Theor.* **45** 215304
- [52] Liu J, Chen W, Zhang B, Zhao J, Wu J, Yuan J and Zhao Z 2014 Trajectory-based analysis of low-energy electrons and photocurrents generated in strong-field ionization *Phys. Rev. A* **90** 063420
- [53] Gong X *et al* 2017 Energy-resolved ultrashort delays of photoelectron emission clocked by orthogonal two-color laser fields *Phys. Rev. Lett.* **118** 143203
- [54] Lindner F, Schatzel M G, Walther H, Baltuska A, Goulielmakis E, Krausz F, Milosevic D B, Bauer D, Becker W and Paulus G G 2005 Attosecond double-slit experiment *Phys. Rev. Lett.* **95** 040401
- [55] Arbo D G, Lemell C, Nagele S, Camus N, Fechner L, Krupp A, Pfeifer T, Lopez S D, Moshhammer R and Burgdorfer J 2015 Ionization of argon by two-color laser pulses with coherent phase control *Phys. Rev. A* **92** 023402
- [56] Huang X, Zhang Q, Xu S, Fu X, Han X, Cao W and Lu P 2019 Coulomb focusing in retrapped ionization with near-circularly polarized laser field *Opt. Express* **27** 38116–24